Proceedings of the Sixth IASTED International Conference
Modelling, Simulation and Identification (MSI 2016)
August 16 - 18, 2016 Campinas, Brazil

A COMPARISON OF DIFFERENT ASSISTANCE STRATEGIES IN POWER ASSISTED WHEELCHAIRS USING AN OPTIMAL CONTROL FORMULATION

Vinicius I. Cuerva, Marko Ackermann, Fabrizio Leonardi
Department of Mechanical Engineering
FEI University
Av. Humberto de Alencar Castelo Branco, No. 3972
São Bernardo do Campo, São Paulo, Brazil
vini.shimoto@gmail.com, mackermann@fei.edu.br, fabrizio@fei.edu.br

ABSTRACT
Power assisted wheelchairs are a promising solution to overcome problems associated with manual wheelchair propulsion, such as the incidence of upper limbs injuries and muscle fatigue. However, there are still open questions regarding the most appropriate assistance strategy. The main goal of this paper is to compare three different types of assistance in power assisted wheelchairs: constant force, proportional force and a novel type of assistance inspired on the impedance control theory. The comparison was performed using a simple model and an optimal control formulation that searched for optimal user actuation and controller parameters so as to minimize the user effort. The fairness of the comparison was ensured by imposing an upper bound on the energy consumption by the motors. The results show that the proportional and impedance control-based strategies are the most appropriate steady state conditions. In typical daily activities such as obstacle avoidance, the impedance control has advantage as it permits a faster system's response.

KEY WORDS
Push-rim activated power wheelchair. optimal control. Wheelchair propulsion. Impedance control. Accessibility. Compliance control.

1. Introduction

Approximately 15% of the global population have some kind of disability [1]. The main factor for this high percentage is the effect of aging because elderly people are more likely to develop injuries.

In Brazil, the demographic census of 2010 released by IBGE (Instituto Brasileiro de Geografia e Estatística) shows that 23.9% of the population (approximately 45 million people) report having some kind of disability, with 7% of the total, or about 14 million people, reporting motor disability [2].In the demographic census of 2000, 10% of people surveyed who reported some type of physical disability are paraplegic, quadriplegic or hemiplegic [3].

Among people with lower limb disabilities, the wheelchair is the most popular means of assistance, providing independence in the activities of daily living [4] however, it has a low mechanical efficiency and, coupled with the repetitive nature of the propulsion movement, it can cause physical injuries on the upper limb joints, particularly on the shoulder [5].

Pushrim-activated power-assisted wheelchairs (PAPAW's) have been proposed to overcome these limitations. This solution provides assistance in manual wheelchairs, without completely replacing manual propulsion, by means of electric motors usually mounted on the rear wheels.

There are at least two types of assistance strategies normally implemented in PAPAW's: the constant assistance, defined by the sign of the user's force applied on the pushrim, and the proportional assistance, that applies a rear wheel torque proportional to the torque applied by the person. An experimental comparison of these two types of assistance strategies is reported in [6]. Other types of power assistance in wheelchairs have been developed aiming at specific activities such as locomotion on ramps and in curves [7], [8] and [9].

There are several experimental studies that compare different manufacturers and types of power assisted wheelchairs [6] or compare their performance with the one of conventional wheelchairs [10]. However, in all these studies subjects had little time to adapt to the tested wheelchairs (like [6] and [11]), which adds to other confounding factors and can hinder a fair comparison.

This study aims at providing a controlled comparison of the idealized propulsion patterns arising for three different assistance strategies in PAPAW's: 1) constant assistance, like those used in the E-motion system (Alber M15); 2) proportional assistance (e.g. [12]); and 3) a novel type of assistance inspired on the impedance control theory (as suggested in [13]). This is achieved using a simple model of wheelchair propulsion and an optimal control formulation, in which user effort is minimized while the energy consumed by the motors is constrained for the three strategies. This is supposed to provide a fair comparison basis.

This paper is structured as follows: section 2 presents the problem formulation with a brief explanation of the

DOI: 10.2316/P.2016.840-042

model used for the dynamic wheelchair/person system, of the model parameters' identification and of the employed optimal control formulation. Section 3 has a brief description of the three assistance strategies investigated in this work: constant, proportional and impedance-based. Section 4 shows the results obtained by solving the optimal control problem for each one the assistance strategies. In section 5, the results are discussed, and in section 6 the conclusions are presented.

2. Problem Formulation

2.1 Dynamic Model

The efficiency of the optimal control simulation is bounded to the model created to represent it so, in order to accurately depict the problem, the model needs to be an accurate mathematically representative of the dynamics of the system wheelchair-person.

As explained in [13], the dynamics of the wheelchair/user system in the sagittal plane, can be modeled using a four-bar-system of rigid bodies, representing the upper arm, the forearm, the rear wheels and the structure of the body and wheelchair, respectively. This model has one degree of freedom in the propulsion phase, and three degrees of freedom in the return phase.

In this study a much simpler model is adopted (Figure1), in line with other studies investigating control strategies ([12], [14] and [15]).

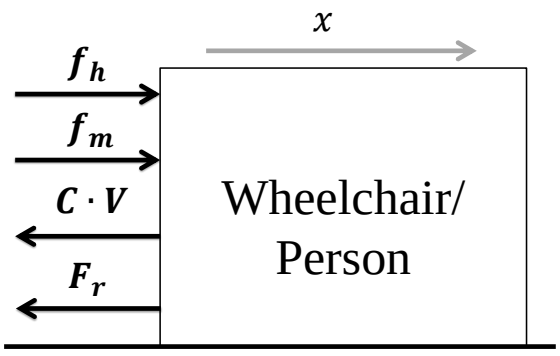

Figure 1. Adopted dynamic model of the system wheelchair/person.

In the model depicted in Figure 1, the dynamic wheelchair/person system is represented by means of a single block with mass M being pushed by forces f_h and f_m, which are the human propulsion and motor forces, respectively. The resistive forces include both, viscous friction force $C \cdot V$ and rolling resistance forces F_r, where C is the viscous damping coefficient and V is the velocity of the wheelchair/person system. x is the longitudinal displacement of the wheelchair.

The governing equations of motion are:

$$\begin{cases} \dot{x} = V \\ f_h + f_m = M \cdot \dot{V} + C \cdot V + F_r \cdot \text{sign}(V) \end{cases} \quad (1)$$

where M, C and F_r are obtained through identification using experimental data, as described in section 2.2.

The dynamics shown in Equation 1 unfortunately doesn't take into account the cyclic characteristic of a wheelchair propulsion. The human propulsion force f_h is assumed to represent the average force over a complete propulsion cycle or to represent the force applied by a caregiver to push the wheelchair along a 10 m track in fixed time so as to grants an average speed of 0.9 m/s. The system will start and stop at rest.

2.2 Model Parameters

The parameters C and F_r were obtained by pushing an E-Motion PAPAW with the assistance turned off together with the user and then releasing the wheelchair so that it decelerates to rest under the exclusive effect of the resistive forces. The speed profile after the releasing (Figure 2) was measured by means of a camera attached to the wheelchair.

Theoretically, when the applied force on the wheelchair was ceased, the reduction of the velocity in the system was caused only by the energy loss due to the damping and the rolling resistance forces. This allowed the estimation of C and F_r using:

$$\begin{bmatrix} V & 1 \end{bmatrix} \cdot \begin{bmatrix} C \\ F_r \end{bmatrix} = -M \cdot \dot{V} \quad (2)$$

where M was adopted as 110 kg, which is the sum of the subject's mass of 77 kg and the mass of the tested PAPAW. The acceleration in Equation 2 was obtained by central differences and the optimal C and F_r values were obtained in a least square differences sense, leading to the following values: $C = 4.5954$ Ns/m and $F_r = 8.8936$ N. The curves in Figure 2 show that the simulated wheelchair response using the estimated parameter values agrees well with the experimental speed profile.

For this work, it was adopted the values: $M = 110\,kg$, $C = 4.6\,Ns/m$ and $F_r = 8.9\,N$.

2.3 Optimal Control Formulation

One of the main concerns regarding the optimal control problem was how to fairly compare the three assistance strategies. This was achieved by limiting the energy consumed by the motor (the work of force f_m) while minimizing the human propulsion effort, quantified by the time integral of the square of the force (f_h). In other words, the human propulsion profile over the 10 m track was determined by minimizing human propulsion effort and the fair comparison was ensured by limiting the energy consumption from the batteries to the same level in the three

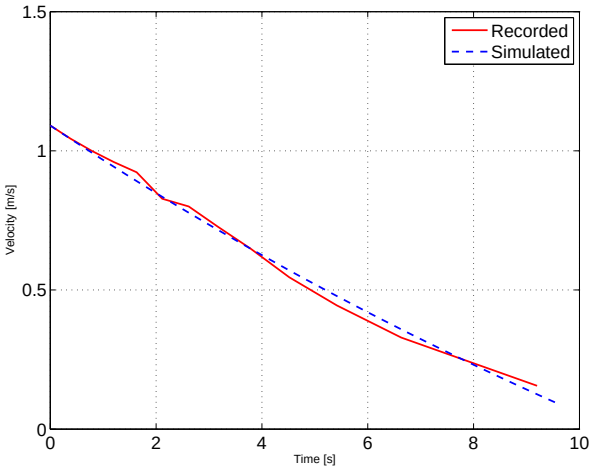

Figure 2. Comparison between the experimental and the simulated results.

cases. We believe this constrained optimization ensures a fair comparison in an ideal situation without interfering on each assistance strategy's peculiarities. The resulting optimal control problem is shown in Equations 3, where t_f is the final time, settled as $10/0.9$ s, $E(f_m, V)$ is the energy consumed by the motor, $W \cdot 3/4$ is the upper bound on the motor's energy consumption (which will be explained further on this section) and $f_m = f_m(f_h)$ represents the control strategy implemented in each case. The energy consumed by the motor from the battery in the deceleration phase, where the work of the motor force is negative, is assumed to be the same amount of energy dissipated during the deceleration phase. This required dividing the optimal control problem into two phases.

A summary of the constraints used in the optimal control problem is shown in Equations 3.

$$
\begin{aligned}
&\min_u J = \int_0^{t_f} f_h^2 \\
&\text{s.t.} \quad \begin{cases} \dot{x} = V \\ \dot{V} = \dfrac{1}{M}\left(f_h + f_m(f_h)\right) - \dfrac{C}{M} \cdot V \\ \qquad - \dfrac{F_r}{M} \cdot \tanh(1000 \cdot V) \end{cases} \\
&E(f_m, V) \leq W \cdot \frac{3}{4} \\
&\dot{V} \in \begin{cases} [0,3] & \text{for acceleration phase} \\ [-3,0] & \text{for decelaration phase} \end{cases} \\
&\begin{cases} x(0) = 0 \\ x(t_f) = 10 \\ V(0) = 0 \\ V(t_f) = 0 \end{cases}
\end{aligned}
\tag{3}
$$

The acceleration of the wheelchair ($\dot{V}$) was constrained to remain within the range $[-3, 3]$ m/s^2 which is a plausible interval for a normal (not an emergency) start/stop [16]. The hyperbolic tangent function was introduced to approximate the sign function in Equation 1 and ensure a continuous model at $V = 0$.

In order to obtain the upper bound on the energy consumed by the motor W, a similar optimal control problem was solved involving the absence of human propulsion ($f_h = 0$ – the actuation is provided exclusively by the motor) and with minimum energy consumption as the optimal function. This solution can be evaluated analytically because the shape of f_m is known: the force f_m is next to infinity at t_0, next to minus infinity at t_f and with a sufficient value in the middle enough to maintain the average speed. This solution creates a constant velocity based equation (Equation 4) which can be evaluated if the average speed of the movement (V_m) is known. x denotes the total distance traveled by the wheelchair.

$$W = M \cdot V_m^2 + C \cdot V_m \cdot x + F_r \cdot x \tag{4}$$

Evaluating for $V_m = 0.9$ m/s, gives $W = 219.5$ J. The constant factor in Equations 3 was adopted based on a common proportional rate of assistance ([6] and [12]).

All the optimal control problems were solved using 200 collocation points and the same initial guess, which is the solution for the optimal control problem in Equation 3 with $f_m = 0$.

In this paper, two commercially available optimal control packages based on the pseudo-spectral method were used: GPOPS-II [17] and PROPT [18]. Another program was developed in MATLAB using the trapezoidal method referred in [19] with the large-scale optimization package IPOPT [20] solver.

3. Assistances Description

3.1 Constant assistance

The first type of assistance (and the most common in the market) is described as a simple constant force applied by the motor when the user applies a torque on the push-rim enough to trigger the assistance. The force and the threshold are both adjustable by the user.

Mathematically, the expression for the motor force (f_m) can be expressed by Equation 5, where K_1 denotes the assistance force applied by the motor and Th is the threshold.

$$f_m(f_h) = \begin{cases} K_1 & \text{if } f_h > Th \\ 0 & \text{if } |f_h| \leq Th \\ -K_1 & \text{if } f_h < -Th \end{cases} \tag{5}$$

The expression in Equation 5 is non-differentiable at Th and $-Th$, which cannot be handled in gradient–based optimization algorithms. A simple solution is to disregard the threshold and approximate the intrinsic sign function in Equation 5, with a hyperbolic tangent, such as shown in Equation 6.

$$f_m(f_h) = K_1 \cdot \tanh f_h \tag{6}$$

The energy spent by the motor is:

$$\begin{aligned} E(f_m, V) &= \int_{t_0}^{t_f} |f_m \cdot V| \quad dt \\ &= \int_{t_0}^{t_f} K_1 \cdot |\tanh f_h \cdot V| \quad dt \\ &\approx \int_{t_0}^{t_f} K_1 \cdot V \quad dt \end{aligned} \tag{7}$$

Because $K_1 > 0$, $V \geq 0$ and $\tanh f_h \approx \text{sign}(f_h)$.

Equations 6 and 7 are both differentiable and do not impose convergence problems to the solver.

3.2 Proportional assistance

In this type of assistance, the motor force follows the shape of the user's force applied on the push-rim, and can be expressed as in Equation 8, where K_2 is the proportional factor.

$$f_m(f_h) = K_2 \cdot f_h \tag{8}$$

This type of assistance was one of the first designed in the literature [12] leading to a PAPAW that is "intuitive" to the user. The function expressed in Equation 8 is continuous and does not impose convergence problems to the NLP solver.

For the proportional assistance, the energy consumed by the motor can be written as function of the user's force as in Equation 9 or, by isolating the person's force in Equation 1, it can be written like in Equation 10.

$$\begin{aligned} E(f_m, V) &= \int_{t_0}^{t_f} |f_m \cdot V| \quad dt \\ &= \int_{t_0}^{t_f} |K_2 \cdot f_h \cdot V| \quad dt \end{aligned} \tag{9}$$

$$\begin{aligned} E(f_m, V) = \int_{t_0}^{t_f} \frac{K_2}{1+K_2} \Big(M \cdot \left|\dot{V}\right| \\ + C \cdot V + F_r \cdot \tanh(1000 \cdot V) \Big) V \quad dt \end{aligned} \tag{10}$$

Because $M, C, K_2, F_r > 0$.

Note that $\dot{V} \geq 0$ in the acceleration phase and $\dot{V} \leq 0$ in the deceleration phase (Equations 3), which makes Equation 10 continuous and differentiable inside the phases where the gradient is needed.

3.3 Impedance assistance

Impedance control is a usual solution to control dynamic systems interacting with the environment and, particularly, with humans. In fact, this strategy is commonly implemented in exoskeletons [21] where there is an interaction between humans and machines. This makes the impedance control a good candidate of assistance strategy in power assisted wheelchairs.

The proposed impedance inspired assistance is shown in Figure 3. If the controller can guarantee a small error e for the range of frequencies that matters to the problem, the strategy can implement a relationship between x and f_r, according to the impedance defined in I.

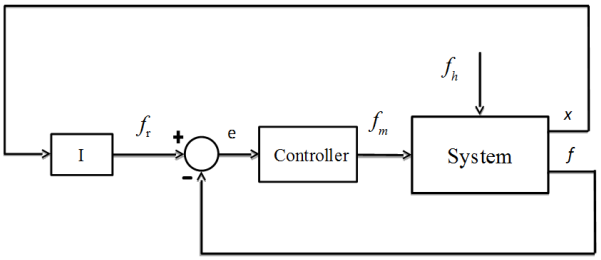

Figure 3. Diagram of the impedance based assistance.

For a SISO system (Single Input-Single Output) and admitting constant and known parameters M, C and F_r, it is possible to write the equations for the impedance method as in Equations 11, which results in a final dynamics seen by the user as in Equation 12, where M_i denotes the apparent mass, C_i the apparent friction coefficient, and F_i the apparent rolling resistance force of the final system. Is important to note that in a real system the parameters M, C and F_r are not accurately known and may vary in time, it will require a robust controller or an adaptive strategy.

$$\begin{cases} f_m = M \cdot \dot{V} + C \cdot V + F_r \cdot \tanh(1000 \cdot V) - f_h \\ f_m = (M - M_i) \cdot \dot{V} + (C - C_i) \cdot V \\ \quad + (F_r - F_i) \cdot \tanh(1000 \cdot V) \end{cases} \tag{11}$$

$$f_h = M_i \cdot \dot{V} + C_i \cdot V + F_i \cdot \tanh(1000 \cdot V) \tag{12}$$

$$[M_i, C_i, F_i]^T \leq [M, C, F_r]^T \tag{13}$$

The energy consumed by the motor is obtained via:

$$\begin{aligned} E(f_m, V) &= \int_{t_0}^{t_f} |f_m \cdot V| \quad dt \\ &= \int_{t_0}^{t_f} \Big[(M - M_i) \cdot \left|\dot{V}\right| + (C - C_i) \cdot V \\ &+ (F_r - F_i) \cdot \tanh(1000 \cdot V) \Big] \cdot V \quad dt \end{aligned} \tag{14}$$

Considering conditions 13, the same situation seen in Equation 10 is presented in Equation 14.

4. Results

Tables 1, 2 and 3 show the optimal results for the cost function J and controller parameters obtained for the three assistance strategies using the three optimal control packages.

Constant assistance		
Program used	$J\ [N^2 \cdot s]$	$K_1\ [N]$
Trapezoidal method	4201.06	16.46
PROPT	4202.05	16.46
GPOPS-II	4193.08	16.46

Table 1. Results found for the constant assistance case.

Proportional assistance		
Program used	$J\ [N^2 \cdot s]$	K_2
Trapezoidal method	2115.98	1.87
PROPT	2124.61	1.85
GPOPS-II	2120.33	1.85

Table 2. Results found for the proportional assistance case.

Impedance assistance		
Program used	$J\ [N^2 \cdot s]$	$M_i\ [kg]$
Trapezoidal	383.02	1.00
PROPT	398.73	1.06
GPOPS-II	398.13	1.02
Program used	$C_i\ [Ns/m]$	$F_i\ [N]$
Trapezoidal	4.60	1.66
PROPT	4.60	1.78
GPOPS-II	4.60	1.78

Table 3. Results found for the impedance assistance case.

Figures 4, 5, 6 and 7 show the optimal position, velocities, user's force and motor force profiles, respectively. There are substantial differences in the computed optimal profiles for the three different control strategies. The optimal response of an assisted wheelchair with a constant strategy is characterized by long acceleration and deceleration phases (see Figure 5). The required large user force leads to large cost function values compared to the other propulsion strategies (Table 1 and Figure 6). The optimal response of an assisted wheelchair with a proportional strategy is characterized by shorter acceleration and deceleration phases and requires lower user effort (Table 2 and Figure 6), particularly in the steady-state phase, when compared to the constant assistance. With this strategy, the motor force follows the user force profile (Figures 6 and 7), leading to larger motor forces in the acceleration and deceleration phases and lower forces in the steady-state phase. The impedance control-based strategy, in turn, leads to the lowest user effort for the same energy consumed from the

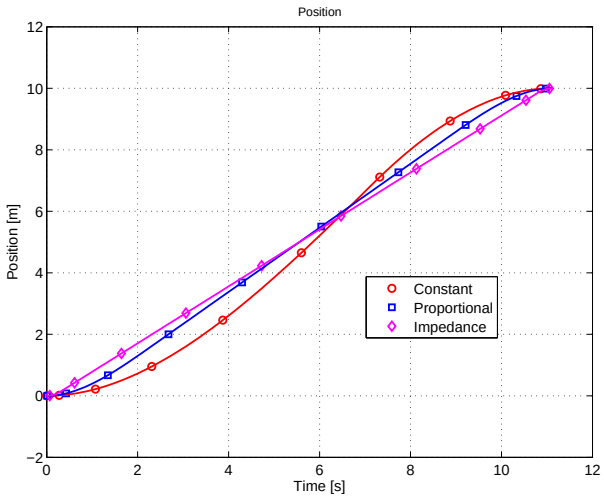

Figure 4. Optimal position profiles for the different types of assistance.

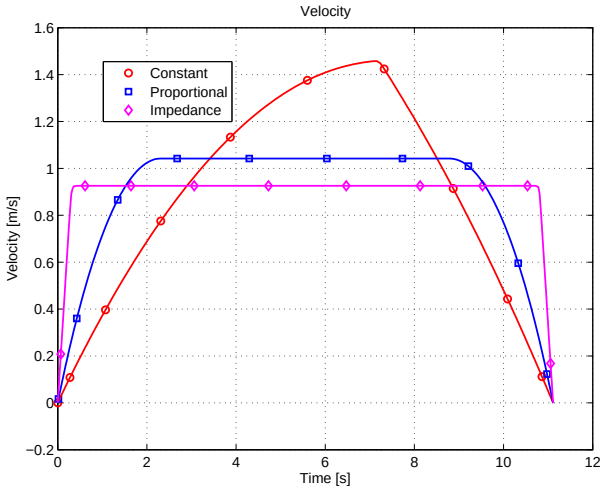

Figure 5. Optimal velocity profiles for the different types of assistance.

battery by the motor in this particular track which reflects the low user forces over the entire trajectory (Table 3 and Figure 6). The resulting optimal motion shows short acceleration and deceleration phases, with a long steady-state phase in which the velocity and user effort remain constant at relatively low levels. This is achieved by large motor force peaks in the short acceleration and deceleration phases (Figure 7), which requires large actuator power.

5. Discussion

All the strategies consumed the same amount of energy from the power supply, as imposed in the optimal control problem, which guaranteed a fair comparison. Despite the same energy expenditure by the motor over the trajec-

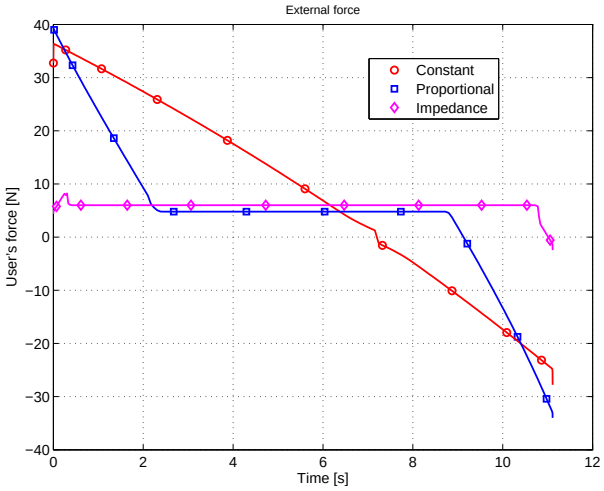

Figure 6. Optimal profile for the user's force for the different types of assistance.

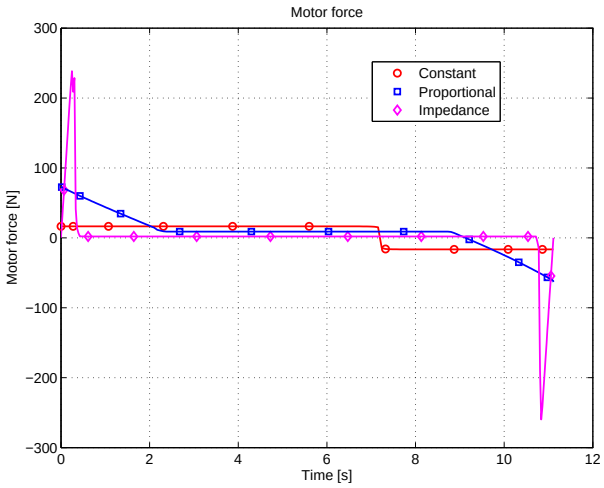

Figure 7. Optimal profile for the motor force for the different types of assistance.

tory, the optimal system behavior changes substantially depending on the implemented assistance strategy. Interestingly, the resulting profiles for the constant assistance and for the impedance control-based assistance resemble typical minimum force and minimum energy profiles, respectively. This indicates that the impedance control-based assistance uses the available energy more efficiently, leading to the lowest user effort among the investigated assistance strategies (Tables 1, 2 and 3).

The constant assistance strategy requires a constant motor force, which needs to be low so that the maximum motor energy expenditure constraint is fulfilled. This implies that a substantial part of the force necessary for accelerating and decelerating the wheelchair originates from the user rather than from the motor. As a consequence, less acceleration is preferable because this reduces the peaks of user force, leading to an almost linear f_h profile (Figure 6).

The proportional assistance strategy, in turn, does not require a constant motor force and permits that a relatively low motor force is applied in the steady-state phase (Figure 6), so that the remaining energy can be employed during acceleration and deceleration, reducing user effort in these phases. This reduction in user force may be interpreted as an apparent reduction in the system parameters M, C and F_r in the equations of motion, i.e. a reduction in system's impedance. However,all of these parameters are always reduced in the same proportion so that the system's time constant M/C remains the same. This is equivalent to saying that the transient system response is not affected by the proportional assistance strategy. Therefore, this assistance strategy is most useful in steady-state conditions where user effort is the lowest (Figure 6), but is probably ineffective in unsteady conditions, which are recurrent in daily activities.

The impedance control-based assistance can be seen as an extension of the proportional control strategy in the sense that it allows altering the system's apparent mass and damping coefficient independently, and thus is able to affect the steady-state as well as the transient system's response. Note, that the damping coefficient C remained the same as the original while the apparent system's mass M_i was altered by a factor of 100 (Table 3), leading to an equivalent reduction in the time constant. This allowed short acceleration and deceleration phases on the expense of large, yet brief, motor force spikes. This feature of the impedance control-based strategy is highly desirable in daily activities, which are far from steady-state, such as indoors propulsion, obstacle avoidance, door opening and other short range maneuvers. On the other hand, in steady-state conditions there is no substantial advantage of the impedance control-based strategy over the proportional strategy.

Both in the proportional and the impedance control-based assistance, the rolling resistance force F_r, due to its constant nature, only shifts the steady-state force, having no influence on the system dynamics (depicted in Figures 4 and 5). The constant assistance is more affected by the rolling resistance due to the similar nature of the assistance and the rolling resistance, which helps in the deceleration phase and is detrimental in the acceleration and steady-state phases.

6. Conclusions

This paper presented a comparison of three assistance strategies in power-assisted wheelchairs: constant, proportional and an impedance control-based assistance. The comparison was performed using an optimal control formulation that searched for optimal user actuation and controller parameters so as to minimize the user effort. The fairness of the comparison was ensured by imposing an upper bound on the energy consumption by the motors.

In spite of the same total energy consumption, optimal patterns differed substantially, with the constant assis-

tance strategy leading to a minimum force motion pattern and the impedance control-based strategy leading to a minimum energy motion pattern. The constant assistance required the largest user effort by requiring a large user actuation in the acceleration and deceleration phases. The proportional assistance allowed a lower steady-state user force but was not able to affect the system's time constant. The impedance control-based strategy, on the contrary, allowed a reduction of the time constant leading to short acceleration and deceleration phases and the lowest user effort, on the expense of large motor force spikes in these phases.

The results presented in this study indicate that in steady-state conditions there are probably small differences between the different control strategies. However, the choice of the control strategy has an important effect on the transient response, typical in daily activities such as obstacle avoidance, indoors propulsion and door opening. In these conditions, the comparison shows a clear superiority of the impedance control-based strategy because it requires lower user effort in the acceleration and deceleration phases as well as allows for a shorter transient time by changing the system's time constant. The price for the superior performance is the larger force spikes necessary to reduce system's apparent impedance in transient conditions, which would probably require larger motors.

One limitation of this paper is the model used. Because of it's nature, it can't represent the propulsion cycle created by the wheelchair's user to push the system by it's own, limiting the resolutions to a situation where the wheelchair/user is being pushed by a caregiver. Future works should test the three types of assistance by using a more complex model, allowing it to analysis the impacts of the assistances on the propulsion cycle or even its consequences on the musculoskeletal system.

References

[1] W. H. OMS, World report on disability, Library Cataloguing-in-Publication Data World report on disability, 2011.

[2] IBGE, Censo demográfico: Características gerais da população, religião e pessoas com deficiência, Rio de Janeiro, Brazil, 2010.

[3] ——, Censo demográfico: características gerais da população, religião e pessoas com deficiência, Rio de Janeiro, 2000.

[4] K. C. Alonso, E. R. F. B. M. Azevedo, E. W. Cacho, R. Varoto, A. Cliquet Júnior *et al.*, Kinematic assessment of transfer of paraplegic subjects from the wheelchair, *Acta Ortopédica Brasileira*, 19(6), 2011, 346–352.

[5] M. G. Kloosterman, J. H. Buurke, W. de Vries, L. H. V. der Woude, and J. S. Rietman, Effect of power-assisted hand-rim wheelchair propulsion on shoulder load in experienced wheelchair users: A pilot study with an instrumented wheelchair, *Medical Engineering & Physics*, 37(10), 2015, 961–968.

[6] B. Guillon, G. Van-Hecke, J. Iddir, N. Pellegrini, N. Beghoul, I. Vaugier, M. Figère, D. Pradon, and F. Lofaso, Evaluation of 3 pushrim-activated power-assisted wheelchairs in patients with spinal cord injury, *Archives of physical medicine and rehabilitation*, 96(5), 2015, 894–904.

[7] S. Oh, N. Hata, and Y. Hori, Control developments for wheelchairs in slope environments, *Proceedings of the American Control Conference*, Portland, USA, 2005, 739–744.

[8] S.-W. Hwang, C.-H. Lee, and Y.-b. Bang, Power-assisted wheelchair with gravity compensation, *12th International Conference on Control, Automation and Systems (ICCAS)*, JeJu Island, Korea, 2012, 1874–1877.

[9] F. O. Medola, B. M. Purquerio, V. Elui, and C. A. Fortulan, Conceptual project of a servo-controlled power-assisted wheelchair, *Biomedical Robotics and Biomechatronics (2014 5th IEEE RAS & EMBS International Conference)*, São Paulo, Brazil, 2014, 450–454.

[10] M. G. Kloosterman, G. J. Snoek, L. H. van der Woude, J. H. Buurke, and J. S. Rietman, A systematic review on the pros and cons of using a pushrim-activated power-assisted wheelchair, *Clinical rehabilitation*, 27(4), 2013, 299–313.

[11] M. G. Kloosterman, H. Eising, L. Schaake, J. H. Buurke, and J. S. Rietman, Comparison of shoulder load during power-assisted and purely hand-rim wheelchair propulsion, *Clinical Biomechanics*, 27(5), 2012, 428–435.

[12] R. A. Cooper, T. A. Corfman, S. G. Fitzgerald, M. L. Boninger, D. M. Spaeth, W. Ammer, and J. Arva, Performance assessment of a pushrim-activated power-assisted wheelchair control system, *IEEE Transactions on Control Systems Technology*, 10(1), 2002, 121–126.

[13] M. Ackermann, F. Leonardi, H. Costa, and A. Fleury, Modeling and optimal control formulation for manual wheelchair locomotion: The influence of mass and slope on performance, *International Conference on Biomedical Robotics and Biomechatronics (2014 5th IEEE RAS & EMBS)*, São Paulo, Brazil, 2014, 1079–1084.

[14] T. Matsui, S. Fujimoto, K. Yoshida, and T. Akagi, Development of power-assisted wheelchair with consideration of driving environment-dynamic estimation of slope angle and adaptive control system

design, *International Journal of Materials Science and Engineering*, 3(1), 2015, 25–30.

[15] S. Oh and Y. Hori, Disturbance attenuation control for power-assist wheelchair operation on slopes, *IEEE Transactions on Control Systems Technology*, 22(3), 2014, 828–837.

[16] A. Karmarkar, R. A. Cooper, H. yi Liu, S. Connor, and J. Puhlman, Evaluation of pushrim-activated power-assisted wheelchairs using ANSI/RESNA standards, *Archives of Physical Medicine and Rehabilitation*, 89(6), 2008, 1191–1198.

[17] M. A. Patterson and A. V. Rao, Gpops-ii: A matlab software for solving multiple-phase optimal control problems using hp-adaptive gaussian quadrature collocation methods and sparse nonlinear programming, *ACM Transactions on Mathematical Software (TOMS)*, 41(1), 2014, 1.

[18] P. E. Rutquist and M. M. Edvall, Propt-matlab optimal control software, *Tomlab Optimization Inc*, 260(1), 2010.

[19] J. T. Betts, *Practical methods for optimal control and estimation using nonlinear programming*. (Philadelphia: Siam, 2010).

[20] A. Wächter and L. T. Biegler, On the implementation of an interior-point filter line-search algorithm for large-scale nonlinear programming, *Mathematical Programming*, 106(1), 2005, 25–57.

[21] K. Anam and A. A. Al-Jumaily, Active exoskeleton control systems: State of the art, *Procedia Engineering*, 41, 2012, 988–994.